Biochimica et Biophysica Acta, 980 (1989) 319–325
Elsevier

BBA 74380

Intermixing of dipalmitoylphosphatidylcholine with phospho- and sphingolipids bearing highly asymmetric hydrocarbon chains

Michael Gardam and John R. Silvius

Department of Biochemistry, McGill University, Montréal (Canada)

(Received 25 October 1988)

Key words: Lipid phase diagram; Interdigitated phase; Phosphatidylcholine; Cerebroside; Sulfatide; Calorimetry

We have used high-sensitivity differential scanning calorimetry to investigate the mixing of dipalmitoylphosphatidylcholine (DPPC) with *N*-lignoceroylgalactocerebroside, *N*-lignoceroylsulfogalactocerebroside and 1-lauroyl-2-lignoceroylphosphatidylcholine. These three lignoceroyl species, whose two hydrocarbon chains are quite discrepant in length, are completely miscible with DPPC in the liquid-crystalline state. Mixtures of all three lignoceroyl lipids with DPPC show phase separation in the gel state, which is observed over a limited range of compositions (from < 10 mol% to just over 40 mol% sulfatide) in the case of *N*-lignoceroylsulfatide and over a wide range of compositions in the cases of *N*-lignoceroylcerebroside (< 10 mol% to > 90 mol% cerebroside) and 1-lauroyl-2-lignoceroyl-PC (roughly 10 mol% to 90 mol% lauroyl/lignoceroyl PC). The extensive solid-solid phase separation observed in mixtures of DPPC and 1-lauroyl-2-lignoceroyl-PC, which show eutectic behavior, is somewhat unexpected given the similar transition temperatures of the two components but appears to reflect the ability of the lignoceroyl species to form an interdigitated gel phase. However, we find no evidence that the *N*-lignoceroylsphingolipids are markedly more prone to segregate laterally in PC-rich bilayers than are previously studied sphingolipid species with shorter *N*-acyl chains. We suggest on the basis of these results that the primary biological importance of the very long *N*-acyl chains found in many sphingolipids may lie in some function other than the promotion of lateral segregation of sphingolipid-enriched domains in biological membranes.

Introduction

It is a striking fact that some of the lipids found in mammalian cell membranes exhibit structures that depart strongly from the 'consensus' pattern exemplified by a diacylglycerophospholipid with acyl chains of roughly equal length. One noteworthy example of this phenomenon is the occurrence in mammalian cell plasma membranes of sphingolipids with *N*-acyl chains whose length greatly exceeds that of the hydrocarbon portion of the sphingosine backbone [1,2]. A variety of 'asymmetric' phospho- and sphingolipids, whose two hydrocarbon chains differ markedly in length, have been reported to form interdigitated phases, in which the longer of the two hydrocarbon chains extends well beyond the bilayer midplane [3–14]. To date, relatively little is known about the effects of this dramatic asymmetry in chain length on the abilities of such lipids to intermix with other lipids whose hydrocarbon chains are more nearly comparable in length. Lateral segregation of interdigitated and noninterdigitated phases has been reported in a few binary lipid systems, including one in which a liquid-liquid as well as solid-solid phase separation has been reported [15–17].

In the light of the above considerations, it is of interest to examine the miscibility of 'asymmetric' lipids, such as the naturally occurring *N*-lignoceroylsphingolipids, with 'symmetric' phospholipids (i.e., phospholipids whose two acyl chains are of similar length) of the type that comprise the major fraction of natural membrane phospholipids. The potential of the former species to form interdigitated phases in isolation [7,10,11,13] could in principle favor their lateral segregation from symmetrical phospholipids in mixed lipid bilayers or even in biological membranes. To test this possibility, we have examined here the mixing of a symmetrical

Abbreviations: 24 : 0-cerebroside, *N*-lignoceroylgalactocerebroside; DPPC, 1,2-dipalmitoylphosphatidylcholine; EDTA, ethylenediaminetetraacetic acid, trisodium salt; Hepes, 4-(2-hydroxyethyl)-1-piperazineethanesulfonic acid; PC, phosphatidylcholine; 12 : 0/24 : 0-PC, 1-lauroyl-2-lignoceroylphosphatidylcholine; 24 : 0-sulfatide, *N*-lignoceroyl-3′-sulfogalactocerebroside.

Correspondence: J.R. Silvius, Department of Biochemistry, McGill University, Montréal, Québec, Canada H3G 1Y6.

phospholipid, dipalmitoylphosphatidylcholine (DPPC), with the highly asymmetric lipids *N*-lignoceroylgalactocerebroside (24 : 0-cerebroside), *N*-lignoceroyl-3′-sulfogalactocerebroside (24 : 0-sulfatide), and 1-lauroyl-2-lignoceroylphosphatidylcholine (12 : 0/24 : 0-PC). A particularly interesting phase diagram is obtained for the DPPC/1-lauroyl-2-lignoceroyl-PC system, which exhibits clear eutectic behavior. However, we find no evidence that the lignoceroyl species examined here are significantly more prone to segregate laterally in a liquid-crystalline phospholipid bilayer than are other lipids with the same headgroups but more nearly symmetrical hydrocarbon chains.

Materials and Methods

Materials. Galactocerebroside and 3′-sulfogalactocerebroside (sulfatide) were isolated from an acetone powder of bovine brain by Folch extraction, then purified by silicic acid and ion-exchange chromatography, using methods described previously [18,19]. *N*-Lignoceroylgalactocerebroside was synthesized from brain cerebroside by alkaline deacylation [20] followed by reacylation with lignoceric acid in the presence of triphenylphosphine and 4,4′-bispyridyldisulfide [21]. *N*-Lignoceroylsulfatide was synthesized starting from bovine brain sulfatide by the procedure of Koshy and Boggs [22,23]. 1-Lauroyl-2-lignoceroylphosphatidylcholine was synthesized, starting from dilauroylphosphatidylcholine, by the procedure of Mason et al. [24]. These lipids were purified by silicic acid column chromatography followed by preparative thin-layer chromatography and a final precipitation from chloroform with cold acetone. Dilauroyl- and dipalmitoylphosphatidylcholine (99 + %) were obtained from Sigma (St. Louis, MO).

Methods. Lipid samples were lyophilized from cyclohexane and dispersed in 156 mM NaCl, 10 mM Hepes, 1 mM EDTA (pH 7.4) by vortexing above the phase transition of the higher-melting component. Samples containing lignoceroylcerebroside, lignoceroylsulfatide or 1-lauroyl-2-lignoceroyl-PC were very briefly heated to 90 °C, to 65 °C or to 60 °C, respectively, then cooled rapidly to 55 °C and cooled from the latter temperature to 4 °C at a rate less than 0.3 C°/min. Except where otherwise explicitly indicated, samples were then incubated at 4 °C for 45 to 60 days before calorimetric analysis.

High-sensitivity differential scanning calorimetric analysis of lipid samples was carried out with a Microcal MC-1 scanning calorimeter, using a scan rate of 12 C°/h. Equilibrated samples (5 μmol total lipid in 0.7 ml buffer) were loaded into the calorimeter at temperatures below 5 °C and were scanned to a temperature at least 10 C° above the transition temperature of the higher-melting lipid component. In some experiments, samples were then recooled to 5 °C at a rate of roughly 1 C°/min and rescanned within 2 h. Concentrations of lipid stock solutions were determined by phosphorus analysis [25] for phosphatidylcholines and by weighing thoroughly dried samples for lignoceroylgalactocerebroside and lignoceroylsulfogalactocerebroside. Phase transition boundaries were estimated from thermograms recorded for mixed-lipid samples using the procedure of Mabrey and Sturtevant [26].

Results

DPPC/lignoceroylcerebroside mixtures

In Fig. 1 are shown a series of calorimetric traces obtained for extensively preincubated samples combin-

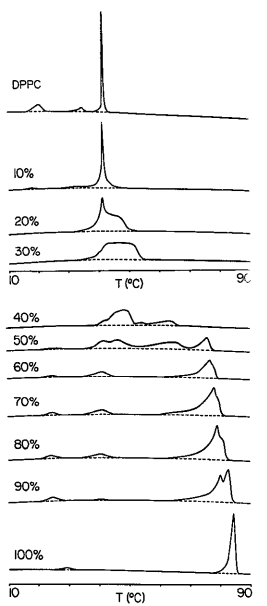

Fig. 1. Heating thermograms recorded for samples combining DPPC with the indicated molar percentages of lignoceroylcerebroside. After initial dispersal as described in Materials and Methods, samples were incubated for 45 days at 4 °C before calorimetric analysis. Other details of the calorimetric analysis were as described in Materials and Methods.

ing DPPC with 24:0-cerebroside in varying proportions. The preparation of DPPC used in these experiments, after incubation for 45 days at 4°C, exhibits sub-, pre- and main transitions at 20.6°C, 35.0°C and 42.0°C, respectively. Pure 24:0-cerebroside preincubated under the same conditions shows a small endotherm at 29.4°C and a large endothermic transition at 85.2°C. Samples of 24:0-cerebroside that were incubated for shorter periods of time (up to 20 days) also showed a second high-temperature transition, centered at 82.9°C (not shown), which is probably the same as the 82°C transition observed by Reed and Shipley [11] in samples of 24:0-cerebroside that were incubated for times on the order of minutes to hours. The amplitude of the 82.9°C transition gradually decreased, while that of the 85.2°C transition increased, as samples were incubated for increasing times at 4°C. The lower-temperature transition of 24:0-cerebroside was not observed in samples that were incubated for short times (hours or a few days) prior to calorimetry.

As increasing amounts of 24:0-cerebroside are incorporated into DPPC bilayers, the main transition of the latter species gradually broadens, with the upper boundary shifting to progressively higher temperatures (Fig. 1). However, the lower boundary of the main transition envelope remains near 41.6°C for mixtures containing as much as 90 mol% 24:0-cerebroside. The pre- and subtransition endotherms observed for DPPC are broadened and shifted to lower temperatures for samples containing 10 mol% cerebroside and cannot be clearly resolved in samples containing 20 mol% or more 24:0-cerebroside. However, an apparently different low-temperature transition is seen at 25.0°C in samples containing 50–90 mol% cerebroside and at 29.4°C in samples containing 100 mol% cerebroside.

In Fig. 2A is shown the phase diagram derived from the data shown in Fig. 1 for the DPPC/24:0-cerebroside system. A horizontal line of three-phase coexistence at 41.6°C extends from < 10 mol% to over 90 mol% DPPC. A second line of three-phase coexistence is clearly present at 25.0°C, extending from < 50 mol% to > 90 mol% 24:0-cerebroside. To account for the observed behavior of the pretransition as 24:0-cerebroside is introduced into DPPC, and noting that DPPC and 24:0-cerebroside are almost completely phase-separated at temperatures just below the main phase transition, we suggest the existence of a third line of three-phase coexistence at a temperature somewhere between 33°C and 25.0°C (plotted tentatively at 33°C on the phase diagram). This putative feature of the phase diagram may not be clearly resolvable in the thermograms of samples containing 20 mol% or more

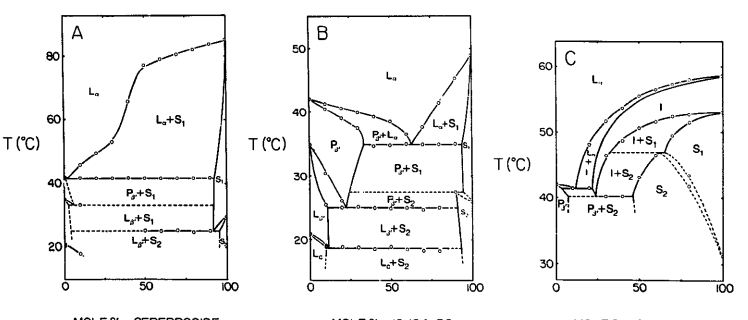

Fig. 2. Phase diagrams deduced from calorimetric data for binary mixtures of DPPC with (A) *N*-lignoceroylgalactocerebroside (24:0-cerebroside), (B) 1-lauroyl-2-lignoceroylphosphatidylcholine (12:0/24:0-PC) and (C) *N*-lignoceroyl-3′-sulfogalactocerebroside (24:0-sulfatide). Phases are designated as follows: L_α, liquid-crystalline; $P_{\beta'}$, 'ripple' phase formed by DPPC between the pre- and main transitions; $L_{\beta'}$, gel phase formed by DPPC between the sub- and pre-transitions; L_c, subgel phase formed by DPPC; S_1, S_2, upper- and lower-temperature solid phases formed by the lignoceroyl species (which may be different for each lignoceroyl lipid examined); I, intermediate phase formed by 24:0-sulfatide between the main and the highest-temperature transition. Data points plotted represent the onset and completion temperatures, estimated using the procedure of Mabrey and Sturtevant [26], for endothermic events associated with regions of two-phase coexistence in the phase diagram, as well as the peak temperatures measured for endothermic features associated with lines of three-phase coexistence. Phase boundaries that can be reliably assigned from the calorimetric data are indicated by solid lines in the phase diagrams,, while boundaries whose position cannot be assigned precisely, or which must be postulated in order to complete the phase diagrams in accordance with the phase rule, are indicated as dashed lines. For clarity, some regions of the phase diagrams are left unlabeled when the phases present can be clearly infered from the labeling of the adjacent regions.

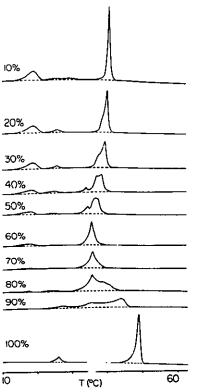

Fig. 3. Heating thermograms recorded for samples of DPPC plus the indicated molar percentages of 12:0/24:0-PC. Samples were dispersed at 60°C and incubated for 45 days at 4°C prior to calorimetry. Other details of sample preparation and calorimetric analysis are given in Materials and Methods.

24:0-cerebroside if the relevant endotherm is relatively broad, since the enthalpy involved is small.

The position of the liquidus curve in the phase diagram in Fig. 2A indicates that DPPC and 24:0-cerebroside are completely miscible, albeit in a highly nonideal manner, in the liquid-crystalline state. The overall behavior of the liquidus curve is quite similar to that observed by Ruocco et al. [27] in the phase diagram for the DPPC/*N*-palmitoylgalactocerebroside system.

DPPC/12:0/24:0-PC mixtures

In Fig. 3 are shown the thermograms recorded for a series of mixtures of DPPC and 12:0/24:0-PC that were incubated for 45 days at 4°C before calorimetric analysis. The effective chain length difference for 12:0/24:0-PC is similar to (albeit slightly greater than) that estimated for lignoceroylsphingolipids [28] and is of the magnitude shown by Xu and Huang [14] to favor the formation of mixed interdigitated phases in the gel state. Pure 12:0/24:0-PC after lengthy preincubation shows a major phase transition at 49.5°C and a smaller phase transition at 26.0°C. The enthalpies of these transitions are 1.4 ± 0.2 and 13.8 ± 0.3 kcal · mol^{-1}, respectively. The larger, but not the smaller transition is also observed in samples that are incubated for shorter times (hours to a few days) at 4°C after heating to 60°C.

As increasing amounts of 12:0/24:0-PC are incorporated into DPPC bilayers, the sub-, pre- and main transitions of the latter species all shift to lower temperatures. The sub- and pretransitions reach new constant temperatures (18.7°C and 25.0°C, respectively) in samples containing > 10 mol% and > 20 mol% 12:0/24:0-PC, respectively. The upper boundary of the main transition gradually shifts downward as the mole percentage of 12:0/24:0-PC is increased from 0 to 60 mol%, then gradually rises again from 70 to 100 mol% 12:0/24:0-PC.

In Fig. 2B is shown the phase diagram derived from the calorimetric data shown in Fig. 3 for the DPPC-12:0/24:0-PC system. Three lines of three-phase coexistence can be definitely assigned, at 18.7°C, 25.0°C and 35.0°C, respectively. A fourth line of three-phase coexistence must be present between 25°C and 35°C to account for the behavior of the low-temperature transition of 12:0/24:0-PC; this three-phase line is tentatively assigned at 27.5°C. A clear eutectic point is seen at 35.0°C, corresponding to a eutectic composition of roughly 63 mol% 12:0/24:0-PC. Phase separation is seen below 35°C in mixtures containing from roughly 35 mol% up to at least 90 mol% 12:0/24:0-PC. Phase separation at lower temperatures, where the DPPC-rich phase enters the $L_{\beta'}$ and L_c phases, is even more extensive. The two lipids are fully miscible in the liquid-crystalline phase.

DPPC/lignoceroylsulfatide mixtures

In Figure 4 are shown a series of thermograms recorded for extensively preincubated dispersions combining DPPC with 24:0-sulfatide in various proportions. Pure 24:0-sulfatide shows a major endothermic transition peaking at 52.8°C, followed by a small transition at 58.5°C. When the sample was cooled rapidly from 65°C after the initial heating run and then immediately rescanned, a similar pattern of endotherms was observed, but the major endotherm in this case was slightly broader and appeared to be the sum of two transitions separated by 1–2 C° (not shown). Given the rich polymorphic behavior observed previously for this and other species of sulfatide using other conditions of sample preparation [13,29,30], this behavior is not surprising. An additional small, relatively broad endotherm is seen, with a peak at 41.8°C, in the thermograms of samples of pure 24:0-sulfatide that are incubated at 4°C for either a few hours or 60 days after dipersal at 65°C. A low-temperature transition has also been reported by Boggs et al. [29] for samples of this lipid dispersed at relatively low salt concentrations.

As increasing amounts of 24:0-sulfatide are incorporated into DPPC bilayers, both the pre- and the sub-transition shift to lower temperatures and become less distinct (Fig. 4). In contrast, the main phase transition of DPPC broadens and gradually shifts to higher tem-

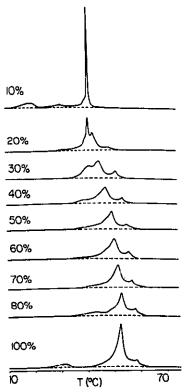

Fig. 4. Heating thermograms recorded for mixtures of DPPC plus the indicated molar percentages of 24:0-sulfatide. Samples were dispersed at 60°C and incubated for 60 days at 4°C prior to calorimetry. Other details of sample preparation and calorimetric analysis were as given in Materials and Methods.

peratures as the proportion of 24:0-sulfatide in the bilayers increases. The lower boundary of the main transition envelope remains near 41°C up to 40 mol% 24:0-sulfatide but then progressively increases as the molar percentage of sulfatide increases still further. Interestingly, the small upper-temperature transition observed for pure 24:0-sulfatide is also observed for mixtures containing as little as 20 mol% sulfatide in DPPC.

In Fig. 2C is shown the phase diagram infered from the above calorimetric results for the DPPC/24:0-sulfatide system. The presence of multiple upper-temperature transitions for 24:0-sulfatide complicates substantially the complete assignment of all features in the phase diagram. However, the position of the liquidus curve, and the limits of the phase separation immediately below 40°C, can be assigned fairly accurately. DPPC and 24:0-sulfatide show a limited region of gel-state immiscibility, extending from < 10 mol% to just over 40 mol% sulfatide. The liquidus curve, which we define from the upper boundary of the high-temperature transition, indicates complete (but not ideal) miscibility of the two lipids in the liquid-crystalline state. The remainder of the phase diagram for this system above 40°C is plotted to rationalize the behavior of the major and the high-temperature transitions in samples containing 20 mol% to 100 mol% 24:0-sulfatide, on the assumption that an intermediate phase (designated 'I') intervenes between the gel and the liquid-crystalline states in these samples. The behavior of the lower-temperature transition of 24:0-sulfatide-rich mixtures is also included in the phase diagram, as phase boundaries related to this transition appear to intersect the solidus curve. However, the pre- and subtransitions of DPPC are not included in this phase diagram, since they cannot be mapped accurately in samples containing 20 mol% or more 24:0-sulfatide but do not appear to be involved in determining the position of the solidus curve.

Discussion

While the formation of interdigitated lamellar phases in a variety of single-component lipid systems is well-documented [3–17,29–37], less is known about the potential for such phases to form in lipid mixtures, particularly in mixtures that contain both lipid species that form interdigitated phases in isolation and species that do not. Coexistence of interdigitated and noninterdigitated gel phases has been observed in the dihexadecyl-PC/dipalmitoyl-PC system [15,16], and Mason [17] has reported intriguing evidence for a limited liquid-liquid phase separation, as well as segregation of interdigitated and noninterdigitated gel phases, in mixtures of distearoyl-PC with 1-stearoyl-2-decanoyl-PC. It has been suggested [9,17] that naturally occurring lipid species with highly discrepant hydrocarbon chain lengths, such as very long-chain sphingolipids, may form segregated interdigitated domains at physiological temperatures in mixed-lipid bilayers and even in some biological membranes. However, little direct evidence has been provided to assess this possibility.

Dipalmitoyl-PC and 12:0/24:0-PC show complete miscibility in the liquid-crystalline state but extensive phase separation in the gel state, leading to the appearance of a eutectic point. The acyl chains of 12:0/24:0-PC show a mismatch in their effective lengths, quantitated by the parameter ($\Delta C/CL$) defined by Huang and Mason [9], of almost exactly 0.5. Xu and Huang [14] have shown that phosphatidylcholines manifesting this degree of acyl chain mismatch form mixed interdigitated bilayers in the gel state. The gel-phase immiscibility observed between 12:0/24:0-PC and DPPC thus presumably reflects the incompatibility of a interdigitated and noninterdigitated gel phases, as has been observed for the dihexadecyl-PC/DPPC and the distearoyl-PC/1-stearoyl-2-decanoyl-PC systems [15–17]. A similar conclusion has very recently been reported by Lin and Huang [47] to explain the eutectic behavior observed in mixtures of dimyristoyl-PC and 1-stearoyl-2-caproyi-PC.

The phase diagram determined for the DPPC/24:0-cerebroside system reveals extensive phase separation in

the gel, but not in the liquid-crystalline state. In view of the results discussed above, it might seem reasonable to conclude that this extensive gel-phase separation is primarily attributable to the incompatibility of a noninterdigitated PC-rich gel phase and an interdigitated gel phase rich in 24:0-cerebroside. However, this conclusion can be questioned on several grounds. First, Ruocco et al. [27] have reported that mixtures of DPPC and *N*-palmitoylcerebroside exhibit phase separation in the gel state over a wide range of compositions. Other PC-cerebroside mixtures, including mixtures of egg PC, DPPC or 1-palmitoyl-2-oleoyl-PC with bovine brain cerebroside, have also been found to exhibit extensive phase separation in the gel state [38–41]. The marked tendency of 24:0-cerebroside to phase-separate from DPPC in the gel state may thus be determined more by its headgroup structure than by its potential to form an interdigitated solid phase. Second, Reed and Shipley [11] have reported evidence that 24:0-cerebroside forms partially interdigitated solid phases, in which neither acyl chain extends completely across the lipid bilayer, rather than mixed interdigitated solid phases, in which the longer acyl chain would span the entire thickness of the hydrocarbon region. It is thus difficult to interpret the phase separation in the DPPC/24:0-cerebroside system as analogous to that observed in mixtures of DPPC with 12:0/24:0-PC, where the gel phase of the lignoceroyl component is expected to adopt a mixed interdigitated structure. The limited solid-solid phase separation that we observe in mixtures of DPPC with 24:0-sulfatide, which forms a mixed interdigitated gel phase [13], likewise cannot be attributed purely to the incompatibility of interdigitated and noninterdigitated gel phases. Rintoul et al. [42] have reported that mixtures of dielaidoyl-PC with natural brain sulfatide, which does not form an interdigitated gel phase [43], show a solid-phase separation that is similar in extent to that observed here for the DPPC/*N*-lignoceroylsulfatide system.

In the liquid-crystalline state 12:0/24:0-PC, 24:0--cerebroside and 24:0-sulfatide are all fully miscible with DPPC. Moreover, the general behavior of the liquidus curve in the phase diagram for the DPPC/24:0-cerebroside system is very similar to that observed previously in the phase diagrams for other PC/cerebroside mixtures [27,38–41], allowing for differences in the transition temperatures of the lipid components in the different systems. It is clear that the lignoceroyl lipid species studied here, with highly discrepant hydrocarbon chain lengths, can readily accommodate to the fluid matrix formed by a symmetric-chain lipid such as DPPC. Grant and co-workers [44,45] have presented evidence that the long acyl chains of several spin-labeled *N*-lignoceroylglycosphingolipids extend across the bilayer midplane, penetrating substantially into the opposing monolayer, when low mole percentages of the sphingolipid labels are incorporated into bilayers composed of symmetrical phospholipids. It would appear from our present results that such interdigitation allows good mixing of lipids with symmetrical and asymmetrical hydrocarbon chains in the liquid-crystalline state. This result agrees with the findings of Grant and co-workers [44,45] that spin-labeled *N*-lignoceroylglycosphingolipids reveal no special tendency to cluster when present at low mole fractions in bilayers of lipids such as egg PC and dimyristoyl-PC.

The phase diagrams presented in this study, when compared to those reported previously for other phospholipid/glycosphingolipid mixtures [27,38–42], provide no evidence that *N*-lignoceroylsphingolipids are markedly more prone to segregate laterally from liquid-crystalline phospholipids than are the corresponding sphingolipids with shorter acyl chains. These results raise some question concerning the suggestion that the primary biological function of the very long *N*-acyl chains of some sphingolipids is to promote the lateral segregation of sphingolipid-enriched domains in the membrane plane. We suggest instead that very long-chain sphingolipids may serve to confer special physical properties (e.g., greater stability or enhanced mechanical coupling between the bilayer leaflets [46]) to the membrane as a whole, or possibly to sphingolipid-enriched domains that may segregate in the membrane plane on the basis of properties other than the length of the lipid acyl chains.

Acknowledgements

This research was supported by grants from the Medical Research Council of Canada and les Fonds F.C.A.R. du Québec. M.G. was the recipient of a Medical Research Council of Canada Studentship award.

References

1 O'Brien, J.S. and Rouser, G. (1964) J. Lipid Res. 5, 339–342.
2 Rouser, G., Nelson, G.J., Fleischer, S. and Simon, G. (1968) in Biological Membranes: Structure and Function (D. Chapman, ed.), pp. 5–70, Academic Press, New York.
3 Mason, J.T., Huang, C.-h. and Biltonen, R. (1981) Biochemistry 20, 6086–6092.
4 Huang, C., Mason, J.T. and Levin, I.W. (1983) Biochemistry 22, 2775–2780.
5 McIntosh, T.J., Simon, S.A., Ellington, J.C., Jr. and Porter, N.A. (1984) Biochemistry 23, 4038–4044.
6 Hui, S.W., Mason, J.T. and Huang, C.-h. (1984) Biochemistry 23, 5570–5577.
7 Levin, I.W., Thompson, T.E., Barenholz, Y. and Huang, C. (1985) Biochemistry 24, 6282–6286.
8 Boggs, J.M. and Mason, J.T. (1986) Biochim. Biophys. Acta 863, 231–243.
9 Huang, C.-h. and Mason, J.T. (1986) Biochim. Biophys. Acta 864, 423–470.
10 Maulik, P.R., Atkinson, D. and Shipley, G.G. (1986) Biophys. J. 50, 1071–1077.

11 Reed, R.A. and Shipley, G.G. (1987) Biochim. Biophys. Acta 896, 153–164.
12 Mattai, J., Sripada, P.K. and Shipley, G.G. (1987) Biochemistry 26, 3287–3297.
13 Boggs, J.M., Koshy, K.M. and Rangaraj, G. (1988) Biochim. Biophys. Acta 938, 373–385.
14 Xu, H. and Huang, C.-h. (1987) Biochemistry 26, 1036–1043.
15 Lohner, K., Schuster, A., Degovics, G., Muller, K. and Laggner, P. (1987) Chem. Phys. Lipids 44, 61–70.
16 Kim, J.T., Mattai, J. and Shipley, G.G. (1988) Biochemistry 26, 6599–6603.
17 Mason, J.T. (1988) Biochemistry 27, 4421–4429.
18 Radin, N.S. (1976) J. Lipid Res. 17, 290–293.
19 Momoi, T., Ando, S. and Magai, Y. (1976) Biochim. Biophys. Acta 441, 488–497.
20 Radin, N.S. (1974) Lipids 9, 358–360.
21 Kishimoto, Y. (1975) Chem. Phys. Lipids 15, 33–36.
22 Koshy, K.M. and Boggs, J.M. (1982) Lipids 17, 998–1000.
23 Koshy, K.M. and Boggs, J.M. (1983) Chem. Phys. Lipids 34, 41–53.
24 Mason, J.T., Broccoli, A.V. and Huang, C. (1981) Anal. Biochem. 113, 96–99.
25 Lowry, R.I. and Tinsley, I.J. (1974) Lipids 9, 491–492.
26 Mabrey, S.J. and Sturtevant, J.M. (1976) Proc. Natl. Acad. Sci. USA 73, 3862–3866.
27 Ruocco, M.J., Shipley, G.G. and Oldfield, E. (1983) Biophys. J. 43, 91–101.
28 Pascher, I. and Sundell, S. (1977) Chem. Phys. Lipids 20, 175–191.
29 Boggs, J.M., Koshy, K.M. and Rangaraj, G. (1984) Chem. Phys. Lipids 36, 65–89.
30 Boggs, J.M., Koshy, K.M. and Rangaraj, G. (1988) Biochim. Biophys. Acta 938, 361–372.
31 McDaniel, R.V., McIntosh, T.J. and Simon, S.A. (1983) Biochim. Biophys. Acta 731, 97–109.
32 Simon, S.A. and McIntosh, T.J. (1984) Biochim. Biophys. Acta 773, 169–172.
33 Braganza, L.F. and Worcester, D.L. (1986) Biochemistry 25, 2591–2596.
34 Hui, S.W. and Huang, C.-h. (1986) Biochemistry 25, 1330–1335.
35 Boggs, J.M. and Rangaraj, G. (1985) Biochim. Biophys. Acta 816, 221–233
36 Boggs, J.M., Stamp, D. and Moscarello, M. (1986) Biochim. Biophys. Acta 863, 231–240.
37 Kubesch, P., Boggs, J.M., Luciano, L., Maass, G. and Tummler, B. (1987) Biochemistry 26, 2139–2149.
38 Maggio, B., Ariga, T., Sturtevant, J.M. and Yu, R.K. (1985) Biochim. Biophys. Acta 818, 1–12.
39 Curatolo, W. (1986) Biochim. Biophys. Acta 861, 373–376.
40 Bunow, M.R. and Levin, I.W. (1988) Biochim. Biophys. Acta 939, 577–586.
41 Johnston, D.S. and Chapman, D. (1988) Biochim. Biophys. Acta 939, 603–614.
42 Rintoul, D.A., Welti, R. and Song, W. (1988) Biophys. J. 53, 126a.
43 Ruocco, M.J. and Shipley, G.G. (1986) Biochim. Biophys. Acta 859, 246–256.
44 Grant, C.W.M., Mehlhorn, I.E., Florio, E. and Barber, K.R. (1987) Biochim. Biophys. Acta 902, 169–177.
45 Mehlhorn, I.E., Florio, E., Barber, K., Lordo, C. and Grant, C.W.M. (1988) Biochim. Biophys. Acta 939, 151–159.
46 Schmidt, C.F., Barenholz, Y., Huang, C. and Thompson, T.E. (1978) Nature 271, 775–777.
47 Lin, H.-n. and Huang, C.-h. (1988) Biochim. Biophys. Acta 946, 178–184.